Video Article

The Generation of Closed Femoral Fractures in Mice: A Model to Study Bone Healing

Justin N. Williams[1], Yong Li[1], Anuradha Valiya Kambrath[1], Uma Sankar[1]

[1]Department of Anatomy and Cell Biology, Indiana University School of Medicine

Correspondence to: Uma Sankar at usankar@iupui.edu

Abstract

Bone fractures impose a tremendous socio-economic burden on patients, in addition to significantly affecting their quality of life. Therapeutic strategies that promote efficient bone healing are non-existent and in high demand. Effective and reproducible animal models of fractures healing are needed to understand the complex biological processes associated with bone regeneration. Many animal models of fracture healing have been generated over the years; however, murine fracture models have recently emerged as powerful tools to study bone healing. A variety of open and closed models have been developed, but the closed femoral fracture model stands out as a simple method for generating rapid and reproducible results in a physiologically relevant manner. The goal of this surgical protocol is to generate unilateral closed femoral fractures in mice and facilitate a post-fracture stabilization of the femur by inserting an intramedullary steel rod. Although devices such as a nail or a screw offer greater axial and rotational stability, the use of an intramedullary rod provides a sufficient stabilization for consistent healing outcomes without producing new defects in the bone tissue or damaging nearby soft tissue. Radiographic imaging is used to monitor the progression of callus formation, bony union, and subsequent remodeling of the bony callus. Bone healing outcomes are typically associated with the strength of the healed bone and measured with torsional testing. Still, understanding the early cellular and molecular events associated with fracture repair is critical in the study of bone tissue regeneration. The closed femoral fracture model in mice with intramedullary fixation serves as an attractive platform to study bone fracture healing and evaluate therapeutic strategies to accelerate healing.

Video Link

The video component of this article can be found at https://www.jove.com/video/58122/

Introduction

Fractures are among the most common injuries occurring to the musculoskeletal system and are associated with a tremendous socioeconomic burden, including treatment costs that are projected to surpass $25 billion annually in the United States[1,2]. Although the majority of fractures heal without incident, healing is associated with substantial downtime and loss of productivity. Approximately 5 - 10% of all fractures result in a delayed healing or non-union, due to age or other underlying chronic health conditions, such as osteoporosis and diabetes mellitus[3,4,5]. No FDA-approved pharmacological treatments are currently available to promote efficient bone healing and shorten recovery time.

Fracture healing is a complex and highly dynamic process involving the coordination of multiple cell types. Hence, a comprehensive understanding of the cellular and molecular events associated with bone regeneration is crucial to the identification of therapeutic targets that accelerate this process. As with other human diseases, the establishment of a highly amenable and reproducible animal model is crucial in the study of bone healing. Larger animals, such as sheep and swine, have bone remodeling properties and biomechanics similar to humans, but are expensive, require substantial healing time, and are not readily amenable to genetic manipulation[6]. On the other hand, small animal models, such as rats and mice, offer many advantages, including an ease of handling, low costs of maintenance, short breeding cycles, and a shorter healing time[7]. Furthermore, the mouse genome is fully sequenced, allowing for the rapid manipulation and generation of genetic variants. Thus, the mouse is a powerful model system to study human disease, injury, and repair[8]. In humans, comorbidities like osteoporosis and diabetes mellitus increase the likelihood of a delayed healing. A number of existing mouse models are available to study the effects of comorbidities such as osteoporosis and diabetes mellitus on bone injury and healing. Patients suffering from osteoporosis have a markedly decreased bone formation during the later stages of a fracture healing[9]. Ovariectomized (OVX) mice exhibit rapid bone loss and delayed bone healing similar to that observed in postmenopausal osteoporosis[10,11]. Additionally, many mouse models of type I and type II diabetes mimic the low bone mass phenotypes and impaired fracture healing seen in humans[11]. Moreover, murine fracture models serve as a versatile platform to study the complex biological processes occurring in the callus and explore novel therapeutic strategies that accelerate bone tissue regeneration.

Despite differences in bone structure and metabolism, the overall process of bone fracture healing remains very similar in mice and humans, involving a combination of endochondral and intramembranous ossification followed by bone remodeling. Endochondral ossification involves the recruitment of progenitor cells to less mechanically stable regions surrounding the fracture gap, where they differentiate into chondrocytes that hypertrophy and mineralize the cartilage to produce a soft callus. The second wave of progenitor cells infiltrate the callus and differentiate into mature osteoblasts that secrete new bone matrix[12,13,14,15]. During intramembranous ossification, progenitors on the periosteal and endosteal

surfaces directly differentiate into matrix secreting osteoblasts and facilitate the bridging of the fracture gap[9,11,12,13]. Together, the endochondral and intramembranous ossifications result in the development of a hard callus, which is further remodeled over time to form a strong secondary bone capable of supporting mechanical loads[13,14,15]. In healthy humans, the healing process takes approximately 3 months, compared to only 35 days in mice[16].

Fracture healing has commonly been studied using either open or closed surgical models[17]. Open surgical approaches, such as the generation of a critically sized defect or complete osteotomy, standardize the injury location and geometry to reduce deviations caused by comminuted fractures. Osteotomies serve as an excellent model to study the underlying mechanism behind a non-union because healing is often delayed compared to closed fractures. Furthermore, a rigid external fixation is required to stabilize the osteotomized bone, meaning the regeneration will primarily depend on the intramembranous ossification. Open surgical approaches use devices such as locking nails, pin-clips, and locking plates to provide axial and rotational stability to the fractured limb; however, such devices are expensive and require significantly more time in surgery[18,19,20,21]. On the other hand, closed models are stabilized with a simple intramedullary fixation device, allowing for enough instability to stimulate endochondral healing. As a result, closed fracture models do not readily mimic the conditions of a non-union. Internal fixation techniques, such as intramedullary pins, nails, and compression screws, are advantageous as they are cheap, easy to use, and minimize the time in surgery[21,22,23]. In some cases, intramedullary pins are inserted prior to the fracture, but the bending of the intramedullary pin can lead to the angulation or displacement of the fractured femur, contributing to a variable callus size and healing. The fracture location and geometry are more difficult to standardize in closed models, as they are generated using a three-point bending device, wherein a weight is dropped on the diaphysis. However, with the proper technique, this surgical approach offers rapid and consistent results. Moreover, the closed fracture model serves as a clinically relevant tool to study fractures caused by high force impact or mechanical stress[22].

This surgical protocol was adapted from previously described methods using an intramedullary pin to stabilize fractured femurs in rats and mice[22,24,25]. First, an intramedullary needle of a small diameter is inserted through the intracondylar notch to establish a point of entry, and a guidewire is introduced prior to generating a transverse fracture at the femoral midshaft using a gravity-dependent three-point bending device. Following the successful generation of a closed femoral fracture, an intramedullary rod of a larger diameter is incorporated over the guide wire to stabilize the fractured femur. This method avoids the risk of delayed healing caused by the angulation of the intramedullary pin during the fracture, as the placement of the rod post-fracture allows for the repositioning and optimized stabilization of the injured femur.

Protocol

The following procedure was performed with approval from the Indiana University School of Medicine Institutional Animal Care and Use Committee (IACUC). All survival surgeries were performed under sterile conditions as outlined by the NIH guidelines. Pain and risk of infections were managed with proper analgesics and antibiotics to ensure a successful outcome.

1. Anesthesia and Preparation

1. Weigh the mouse and anesthetize it with a mixture of ketamine (100 mg/kg) and xylazine (10 mg/kg) administered *via* the intraperitoneal (I.P.) route. Place the mouse in an empty cage and monitor it until it is fully sedated.
2. Ensure that the mouse is sedated using a toe pinch reflex. Apply ophthalmic ointment to its eyes to protect them from drying out.
3. Remove the fur from the right limb. Wipe down the surgical site with an iodine-based scrub and 70% ethanol. Scrub the surgical site starting at the center of the knee and making a circular sweep outward. Repeat this 3x with fresh scrubs, ending with 70% ethanol.
4. Administer a preoperative dose of buprenorphine hydrochloride analgesia (0.03 mg/kg) subcutaneously for the immediate postoperative pain management.
5. Place the mouse on a heating pad covered by a sterile surgical pad.

2. Surgical Approach

NOTE: Prior to the fracture, the weight and the drop height should be empirically determined for the specific strain, age, and sex of the mice prior to the surgery. This surgical procedure is optimized for C57BJ6 male mice at 10 weeks of age.

1. Place the mouse on its back and flex the knee of the operative leg. Using a scalpel blade, make a 1.5 cm incision centered over the knee joint.
2. Laterally displace the patella using forceps to expose the distal end of the femur. Insert a 1.5-in long 25-gauge stainless steel hypodermic needle at the center of the trochlear groove, down the length of the medullary canal in a retrograde manner and through the proximal end of the femur. Take an X-ray to ensure the proper placement of the pin.
   NOTE: The needle should exit the dorsal side of the mouse to create a path for the guidewire.
3. Pass a 4-in long 36-gauge tungsten guidewire through the shaft of the needle, entering through the hub at the distal femur and exiting the bevel on the dorsal side of the mouse.
4. Following the successful placement of the guidewire, carefully remove the 25-gauge needle by gently pulling on the hub while holding the limb and the guidewire in place. Confirm the placement of the guidewire by X-ray.
5. Hold a 391 g weight from a height of 34.6 cm above the impact disc (**Figure 1A**). Position the femur horizontally across the two supporting points, such that the intertrochanteric and supracondylar regions of the femur rest on the support anvils (**Figure 1B**) and the lateral side of the limb is facing the loading point (**Figure 1C**). Drop the weight and carefully remove the mouse from the device immediately following the fracture.
6. Confirm the fracture location by X-ray.
7. Insert the 24-gauge stainless steel hypodermic tubing over the guidewire to stabilize the fractured femur.
   NOTE: This application may require some force as the point of entry was generated using a needle of a smaller diameter. This difference in diameter effectively prevents a potential migration of the 24-gauge rod through the proximal end of the femur. The depth of insertion can be felt manually as the blunt tubing meets the cortical bone of the greater trochanter.

8. Confirm the position of the steel rod and the stabilization of the fractured femur by X-ray before removing the guidewire.
9. Cut the excess tubing at the distal end of the femur using wire cutters. Bury the exposed tubing under the surface of the condyles using forceps to apply a gentle downward force, being careful not to dislocate the knee joint.
10. Reposition the patella using forceps. Close the incision site with a 5-0 absorbable suture.

3. Postoperative Management

1. Following surgery, the mice may be injected with up to 500 µL of sterile saline *via* the I.P. route to aid them in their postoperative recovery.
2. Monitor the animals on a heated recovery bed until they awaken from surgery. Once ambulatory, return them to their cage.
3. Continue to closely monitor the mice for several days after the surgery to ensure they are healing properly and regain mobility. Administer buprenorphine hydrochloride analgesia (0.03 mg/kg) subcutaneously every 6 h for 3 days following the surgery, and as needed thereafter. Avoid the use of non-steroidal anti-inflammatory drugs (NSAIDs) as they have been shown to impair bone healing after surgery.

Representative Results

The successful implementation of the surgical procedure was monitored with radiographic imaging. Key steps include the insertion of an intramedullary needle, the placement of a guide wire, the induction of a transverse fracture at the femoral midshaft, and the proper stabilization with an intramedullary rod (**Figure 2Ai** - **2Aiv**). The healing progression of the fracture callus was monitored with weekly radiographic images up to 28 days following the surgery (**Figure 2B**). At days 10 - 16 post-fracture, the chondrocytes underwent hypertrophy and produced mineralized cartilage to form a prominent soft callus.

Understanding the early cellular and molecular events involved in the endochondral and intramembranous ossifications is important when studying bone fracture healing. Femurs were stained with toluidine blue at 7 and 14 days post-fracture to visualize the formation of a cartilage matrix at the fracture gap (**Figure 3A**). The cartilage formation was detectable 7 days after the fracture and aligned with the fracture gap by day 14 post-fracture.

Following the formation of the soft callus, osteoclasts resorbed calcified cartilage, and mature osteoblasts synthesized new bone matrix. Initially, the bone matrix deposition within the callus was spatially non-specific, but a remodeling of the calcified cartilage, over time, produced more defined structures in the central region and periphery of the fracture callus. Type 1 collagen (COL1) is a major component of bone matrix, and its expression showed the spatial organization and relative amount of bone matrix that was present 14 days post-fracture (**Figure 3B**). Taken together, these data show the coordinated production of cartilage and primary bone matrix during the endochondral healing.

Thereafter, during days 17 - 35 post-fracture, the primary bone was gradually remodeled to form a strong secondary bone resembling that of the cortical midshaft[12]. Microcomputed tomography (micro-CT) analysis revealed the callus volume decreased by approximately 50% between days 14 and 28 post-fracture, indicating an effective remodeling of the callus (**Figure 4A** - **4B**). Although radiographic imaging techniques provide a valuable assessment of the bone content and microarchitecture, torsional testing should be performed to properly assess the bone strength relative to the non-injured contralateral femur.
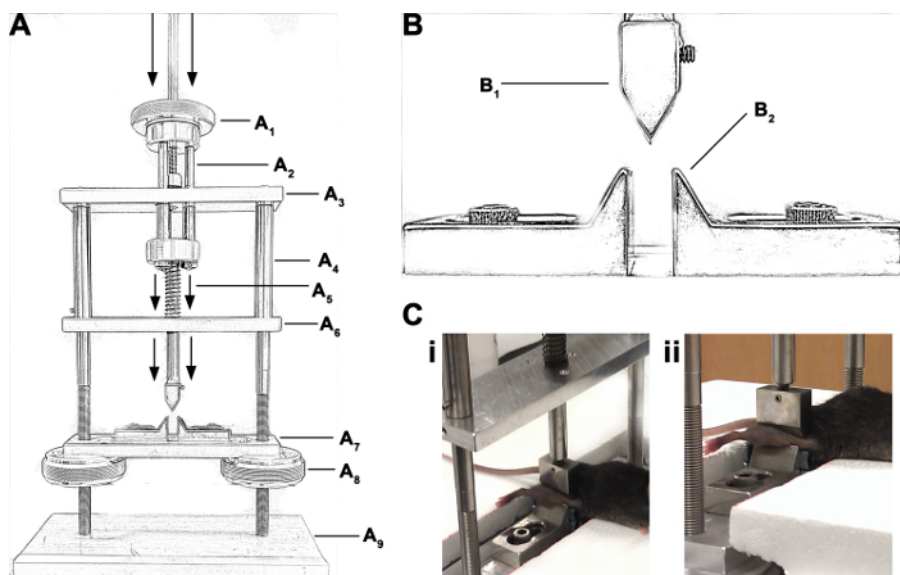

Figure 1: A diagram of the fracture apparatus and the placement of the mouse during the generation of a fracture. (**A**) This panel shows a diagram of the apparatus used to generate fractures and an identification of the components: (**A₁**) the impact disc, (**A₂**) nuts and threaded rods, (**A₃**) the upper platform, (**A₄**) vertical posts, (**A₅**) the spring and shank, (**A₆**) the lower platform, (**A₇**) the support stage, (**A₈**) the knurled knob, and (**A₉**) the base. The arrows indicate a downward displacement of the threaded rods and shank after a weight is dropped onto the impact disc. (**B**) Fractures are generated at the mid-diaphysis using a (**B₁**) guillotine blade while the intertrochanteric and supracondylar regions of the femur are supported by (**B₂**) anvils. (**C**) These images demonstrate the positioning of the mouse hind limb across the support anvils prior to the generation of a fracture. Please click here to view a larger version of this figure.
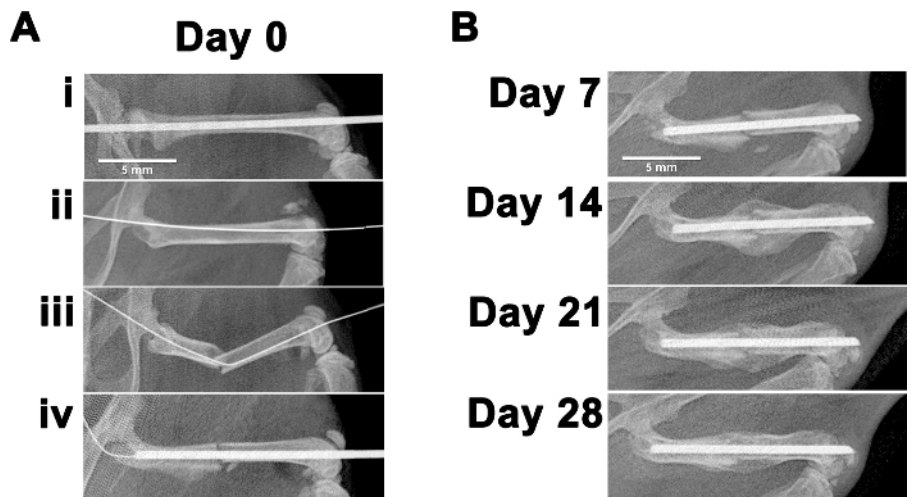
Figure 2: Fracture induction and healing progression monitored with the use of radiography. (**A**) Radiographic images of the mice were taken throughout the surgery showing (**Ai**) the insertion of a 25-gauge needle retrograde through the length of the femur, (**Aii**) the placement of the 30-gauge tungsten guidewire prior to (**Aiii**) the generation of a transverse fracture, and (**Aiv**) the stabilization of the fractured femur with a 24-gauge rod. (**B**) Weekly radiographic images were used to monitor the progression of the healing up to 28 days post-fracture. Please click here to view a larger version of this figure.
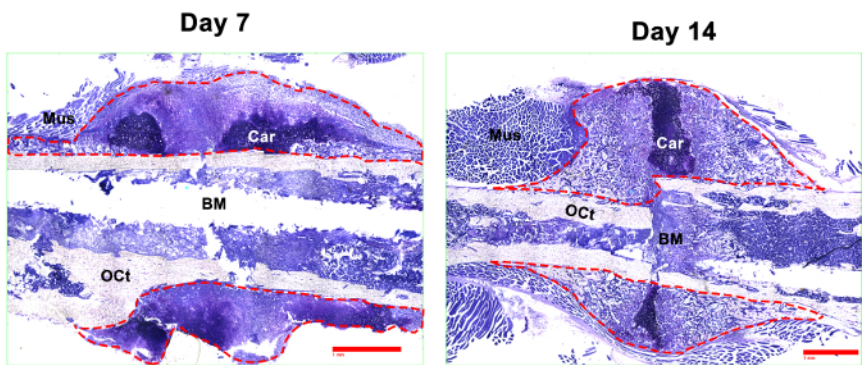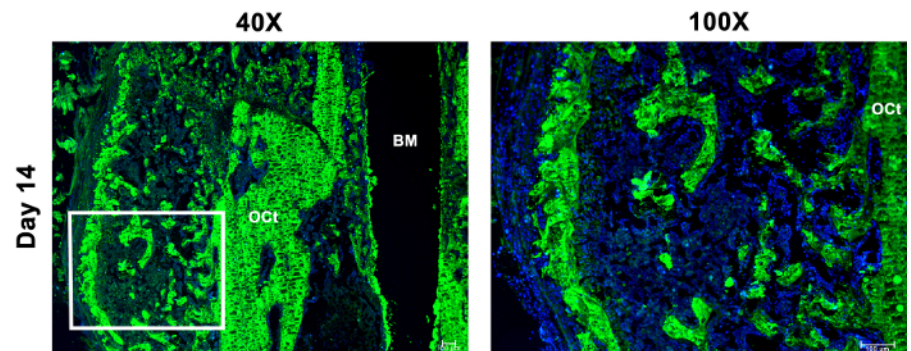

Figure 3: Cartilage formation and new bone matrix deposition during endochondral ossification. (**A**) This panel shows histological sections of 7- and 14-day old calluses stained with toluidine blue. The callus periphery is outlined in red. (**B**) This panel shows the immunohistochemistry staining for the collagen type 1 expression as green inside the fracture callus 14 days post-fracture (40X and 100X magnification). The samples were counterstained with DAPI to visualize nuclei as blue. Car = cartilage; BM = bone marrow; Oct = old cortical bone; Mus = muscle. Please click here to view a larger version of this figure.
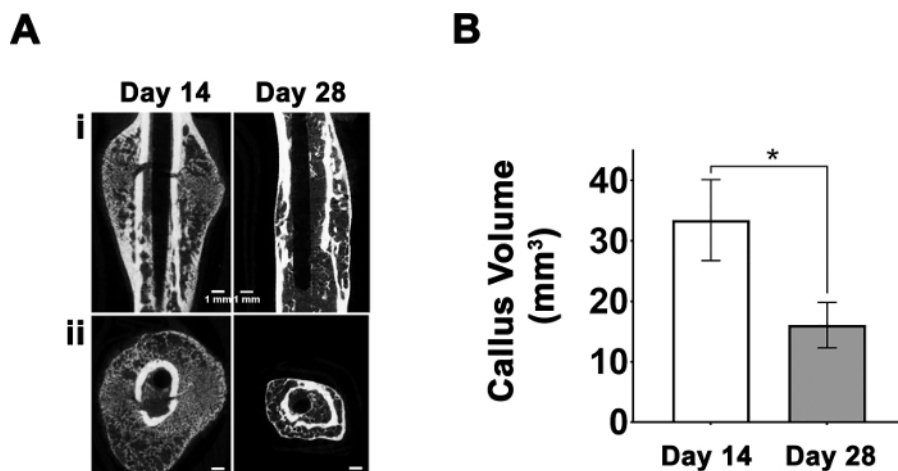
Figure 4: Micro-CT analysis of the fracture callus. (**A**) This panel shows longitudinal and cross-sectional micro-CT images of the fracture callus at 14 and 28 days post-fracture ($n = 6$/group). (**B**) This panel shows the mean callus volume (mm^3) at 14 and 28 days post-fracture. The error bars represent a standard deviation. The statistical comparison among the treatment groups was performed using an unpaired 2-tailed Student's t-test. Standard deviation; * $p < 0.05$. Please click here to view a larger version of this figure.

Discussion

The goal of this surgical procedure is to generate standardized closed femoral fractures in mice. A key advantage of this model is that the internal fixation takes place after the generation of the fracture, thereby avoiding an angulation of the intramedullary rod. Perhaps the most critical aspect of this protocol is the generation of a standardized transverse fracture at the femoral midshaft, as the fracture geometry is dependent on the applied bending force and the positioning of the hind limb. Improper positioning of the femur during the bending moment can lead to oblique or comminuted fractures. The weight and drop height must be empirically predetermined, as they are dependent on the age, sex, and strain of the mice. The applied force can be further controlled using a material testing machine fitted with a three-point bending apparatus in place of a dropped weight[24]. However, generating fractures with a dropped weight is a clinically relevant model of high-impact or stress-related injuries.

In addition, complications may develop during the surgical procedure. The guidewire may become dislocated after the generation of the fracture, leading to a misalignment of the injured femur during the stabilization with the intramedullary rod. This can be prevented by monitoring with radiographic imaging before and after the generation of the fracture. In the case of comminuted fractures, the animal should be excluded from the study. Furthermore, animals should be monitored closely after the surgery for the migration of the intramedullary rod, as this could affect the mobility and the healing of the injured limb. One limitation of the technique is that *in vivo* micro-CT or magnetic resonance imaging (MRI) analyses are not possible, as the stainless steel intramedullary rod would compromise the image quality. Therefore, these analyses can only be performed *ex vivo*, following the careful removal of the intramedullary rod.

Although there are many murine fracture models, the closed femoral fracture model stands out as a simple, efficient, and clinically relevant method to study bone regeneration. The internal fixation with an intramedullary rod, as described in this protocol, provides sufficient stability for consistent bone healing, but may still allow for some degree of axial and rotational movement of the injured femur. While open models such as osteotomies allow for the generation of standardized "fractures," they require a rigid external fixation of the bone, and the healing relies on intramembranous ossification. Acute long bone fractures typically heal through a combination of endochondral and intramembranous ossification. Therefore, the closed femoral fractures described in this protocol provide a physiologically relevant model to study the underlying mechanism of bone healing. Future studies involving murine closed femoral fractures would benefit from the development of a radiolucent intramedullary rod to allow for *in vivo* imaging techniques, such as the use of contrast dyes to measure the formation of new vasculature in the injured limb. Altogether, the murine closed femoral fracture model is an attractive platform to study the cellular and molecular events associated with bone injury and regeneration and identify novel therapeutic targets to accelerate bone healing.

Disclosures

The authors of this manuscript have nothing to disclose. The authors further state that there are no restrictions on the full access to all the material used in the study reported in this manuscript.

Acknowledgements

References

1. Schnell, S., Friedman, S. M., Mendelson, D. A., Bingham, K. W., Kates, S. L. The 1-Year Mortality of Patients Treated in a Hip Fracture Program for Elders. *Geriatric Orthopaedic Surgery & Rehabilitation.* **1** (1), 6-14 (2010).
2. Burge, R. *et al.* Incidence and economic burden of osteoporosis-related fractures in the United States, 2005-2025. *Journal of Bone and Mineral Research.* **22** (3), 465-475 (2007).
3. Cunningham, B. P., Brazina, S., Morshed, S., Miclau, T., III. Fracture healing: A review of clinical, imaging and laboratory diagnostic options. *Injury.* **48**, S69-S75 (2017).
4. Einhorn, T. A. Can an anti-fracture agent heal fractures? *Clinical Cases in Mineral and Bone Metabolism.* **7** (1), 11-14 (2010).
5. Hak, D. J. *et al.* Delayed union and nonunions: epidemiology, clinical issues, and financial aspects. *Injury.* **45 Suppl 2**, S3-S7 (2014).
6. Decker, S., Reifenrath, J., Omar, M., Krettek, C., Muller, C. W. Non-osteotomy and osteotomy large animal fracture models in orthopedic trauma research. *Orthopaedic Reviews* (Pavia). **6** (4), 5575 (2014).
7. Histing, T. *et al.* Small animal bone healing models: standards, tips, and pitfalls results of a consensus meeting. *Bone.* **49** (4), 591-599 (2011).
8. Jacenko, O., Olsen, B. R. Transgenic mouse models in studies of skeletal disorders. *Journal of Rheumatology Supplement.* **43**, 39-41 (1995).
9. Nikolaou, V. S., Efstathopoulos, N., Kontakis, G., Kanakaris, N. K., Giannoudis, P. V. The influence of osteoporosis in femoral fracture healing time. *Injury.* **40** (6), 663-668 (2009).
10. Bain, S. D., Bailey, M. C., Celino, D. L., Lantry, M. M., Edwards, M. W. High-dose estrogen inhibits bone resorption and stimulates bone formation in the ovariectomized mouse. *Journal of Bone and Mineral Research.* **8** (4), 435-442 (1993).
11. Haffner-Luntzer, M., Kovtun, A., Rapp, A. E., Ignatius, A. Mouse Models in Bone Fracture Healing Research. *Current Molecular Biology Reports.* **2** (2), 101-111 (2016).
12. Einhorn, T. A., Gerstenfeld, L. C. Fracture healing: mechanisms and interventions. *Nature Reviews in Rheumatology.* **11** (1), 45-54 (2015).
13. Schindeler, A., McDonald, M. M., Bokko, P., Little, D. G. Bone remodeling during fracture repair: The cellular picture. *Seminar in Cellular and Developmental Biology.* **19** (5), 459-466 (2008).
14. Ai-Aql, Z. S., Alagl, A. S., Graves, D. T., Gerstenfeld, L. C., Einhorn, T. A. Molecular mechanisms controlling bone formation during fracture healing and distraction osteogenesis. *Journal of Dental Research.* **87** (2), 107-118 (2008).
15. Gerstenfeld, L. C. *et al.* Three-dimensional Reconstruction of Fracture Callus Morphogenesis. *Journal of Histochemistry & Cytochemistry.* **54** (11), 1215-1228 (2006).
16. Marsell, R., Einhorn, T. A. Emerging bone healing therapies. *Journal of Orthopaedic Trauma.* **24 Suppl 1**, S4-S8 (2010).
17. Lybrand, K., Bragdon, B., Gerstenfeld, L. Mouse models of bone healing: fracture, marrow ablation, and distraction osteogenesis. *Current Protocols of Mouse Biology.* **5** (1), 35-49 (2015).
18. Garcia, P. *et al.* The LockingMouseNail--a new implant for standardized stable osteosynthesis in mice. *Journal of Surgical Research.* **169** (2), 220-226 (2011).
19. Histing, T. *et al.* An internal locking plate to study intramembranous bone healing in a mouse femur fracture model. *Journal of Orthopaedic Research.* **28** (3), 397-402 (2010).
20. Garcia, P. *et al.* A new technique for internal fixation of femoral fractures in mice: impact of stability on fracture healing. *Journal of Biomechistry.* **41** (8), 1689-1696 (2008).
21. Holstein, J. H. *et al.* Advances in the establishment of defined mouse models for the study of fracture healing and bone regeneration. *Journal of Orthopaedic Trauma.* **23** (5 Suppl), S31-S38 (2009).
22. Bonnarens, F., Einhorn, T. A. Production of a standard closed fracture in laboratory animal bone. *Journal of Orthopaedic Research.* **2** (1), 97-101 (1984).
23. Holstein, J. H., Menger, M. D., Culemann, U., Meier, C., Pohlemann, T. Development of a locking femur nail for mice. *Journal of Biomechistry.* **40** (1), 215-219 (2007).
24. McBride-Gagyi, S. H., McKenzie, J. A., Buettmann, E. G., Gardner, M. J., Silva, M. J. Bmp2 conditional knockout in osteoblasts and endothelial cells does not impair bone formation after injury or mechanical loading in adult mice. *Bone.* **81**, 533-543 (2015).
25. Williams, J. N. *et al.* Inhibition of CaMKK2 Enhances Fracture Healing by Stimulating Indian Hedgehog Signaling and Accelerating Endochondral Ossification. *Journal of Bone and Mineral Research.* (2018).